SHELF-BASIN CONNECTIVITY DRIVES DISSOLVED Fe AND Mn DISTRIBUTIONS IN THE WESTERN ARCTIC OCEAN

A SYNOPTIC VIEW INTO POLAR TRACE METAL CYCLING

By Laramie Jensen and Manuel Colombo

ABSTRACT. There have been many changes over the past few decades in the physical environment and ecosystem health of the Arctic Ocean, which is a sentinel of global warming. Bioactive trace metal data of important micronutrients for algae across the global ocean, such as iron (Fe) and manganese (Mn), are key indicators of biogeochemical change. However, trace metal data in the Arctic have been historically sparse and generally confined to ice-free regions. In 2015, three major GEOTRACES expeditions sought to resolve trace metal distributions across the Arctic, covering the western, eastern, and Canadian Arctic sectors. The diverse Arctic shelves displayed unique controls on Fe and Mn cycling due to differing chemical, biological, and physical properties. Here, we contrast the shallow, reducing Chukchi Shelf in the western Arctic with the tidally forced, advective Canadian Arctic and the deeper, less productive Barents Shelf in the eastern Arctic. Reductive dissolution and physical resuspension both proved to be large sources of Fe and Mn to the Arctic and the North Atlantic outflow. In the isolated intermediate and deep waters, one-dimensional scavenging in the western and eastern Arctic contrasts with vertical biological signals in Baffin Bay and the Labrador Sea.

INTRODUCTION

In 1979, the interdisciplinary Lomonosov Ridge Experiment (LOREX79) set up camp on ice floes near the North Pole, allowing them to drift with the ice across the central Arctic. By drilling holes in the ice, clean Go-Flo bottles (coated in Teflon, with no inner spring mechanism) could be lowered via stainless steel cables to collect water at various points in the water column. While painstaking, this methodology yielded a singular profile that included zinc (Zn), cadmium (Cd), copper (Cu), and aluminum (Al), among other chemical parameters such as radionuclides, oxygen isotopes, and macronutrients (Moore, 1981; Moore et al., 1983). Other such ice station studies quickly followed, including the 1980 Ymer 80 expedition that collected profiles above 84°N for Cd, Cu, nickel (Ni), iron (Fe), and Zn (Danielsson and Westerlund, 1983). By the late 1980s, multiple under-ice trace metal profiles across the four major Arctic basins had been collected (Yeats, 1988). These early studies revealed, for the first time, the impact that fresh, river-derived surface waters, and mixing between nutrient-rich Pacific waters and nutrient-poor Atlantic waters, have on trace metal distribution.

Over the following decades, ships returned to the Arctic to sample water and obtained long-term records for radiocarbon, atmospheric tracers, oxygen isotopes, and macronutrients. However, it was not until the early 2000s that high resolution (vertically and spatially) trace metals were sampled in the central Arctic as part of the International Polar Year (2007–2008). Trace metal sampling techniques and analytical methods had been vastly improved in the interim, leading to a global boom in trace metal studies, greatly boosted by the international GEOTRACES program. Capitalizing on renewed interest in the biogeochemistry of the Arctic, GEOTRACES organized three cruises in 2015 covering the western, eastern, and Canadian sectors of the Arctic (Figure 1).

The Arctic Ocean is particularly vulnerable to the effects of global warming; rapidly increasing air and surface water temperatures result in melting sea ice, increased river discharge, and thawing permafrost, among other disruptions (Frey and McClelland, 2009; Perovich and Richter-Menge, 2015; Holmes et al., 2021). In turn, physical changes to water mass movement and structure are occurring, including an increase in surface stratification and longer periods of ice-free "open" waters (Barnhart et al., 2016; Nummelin et al., 2016). Changes to nutrient supply, phytoplankton community composition, and primary production are already underway (Huntington et al., 2020; Lewis et al., 2020). While ongoing monitoring of sea ice extent, thickness, water circulation, and variability can be done over vast regions and year-round, biogeochemical data have been historically sparse in the Arctic Ocean due to environmental and sampling constraints. As many physical changes to Arctic circulation are expected to have cascading effects on biogeochemical fluxes in and out of the Arctic (Macdonald et al., 2015; Huntington et al., 2020), it is essential to gain a comprehensive understanding of how Arctic geochemistry is changing.

Understanding the sources and fate of trace metals in oceanic ecosystems is vitally important, as they are indicators of significant biogeochemical processes (i.e., scavenging, dust deposition, circulation, sediment resuspension) that occur throughout the water column (Moore and Braucher, 2008; Klunder et al., 2012a; John and Conway, 2014; Whitmore et al., 2020). Bioactive trace metals that are essential micronutrients for phytoplankton in the global ocean (e.g., Fe, Mn, Zn) may limit primary production in surface waters or influence community composition (Morel, 2008; Twining and Baines, 2013). Typical sources of trace metals to the ocean include rivers, atmospheric deposition, continental margins, hydrothermal venting, and recycling of organic matter in the water column (Bruland et al., 2014). Eleven percent of global river discharge takes place in the Arctic, and 54% of its surface is underlain by extensive continental shelves (Opsahl et al., 1999; Jakobsson et al., 2004), making it a particularly interesting and dynamic area for the study of trace metal biogeochemistry.

The connection between river water input and the large, shallow continental shelves in the enclosed Arctic has already been well documented as a bridge between high-latitude terrestrial and marine ecosystems (Carmack et al., 2015). However, each Arctic shelf profiled by the GEOTRACES program in 2015 is unique in its physical and biogeochemical characteristics. In the western Arctic, the Chukchi Shelf is heavily influenced by Pacific water flowing through the Bering Strait and by sea ice formation; the Canadian Arctic Archipelago (CAA) is affected by freshwater input and strong tidal currents; and the Barents Shelf in the Eurasian Arctic modifies inflowing North Atlantic waters. Although we discuss major findings from the GEOTRACES program concerning the different physical and chemical characteristics that influence trace metal sources and fates in the Arctic, our focus here is on dissolved Fe and Mn in the western and Canadian Arctic (GN01, GN02, GN03 cruises; Figure 1a).

HYDROGRAPHY

The Arctic Ocean is an enclosed basin with limited points of exchange between the Atlantic and Pacific Oceans. As a polar ocean, density and stratification are determined primarily by salinity, leading to fresh and cold waters overlying warmer and saltier waters (Rudels, 2015). Submarine ridges separate the Arctic into four major sub-basins: the Canada Basin, the Makarov Basin, the Amundsen Basin,

FACING PAGE. The northern lights (aurora borealis) dance above US Coast Guard Cutter *Healy*. The ship was in the Beaufort Sea, returning from the North Pole, in October 2015 as part of the US Arctic GEOTRACES program. *Photo credit: Coast Guard Petty Officer 2nd Class Corey J. Mendenhall*

and the Nansen Basin. The first two are part of the "western" Arctic, while the latter two are in the "eastern" Arctic. Warm, saltier (~34.9) Atlantic waters enter the eastern Arctic through the Fram Strait (sill depth ~2,600 m) and Barents Sea Opening (~230 m; Figure 1), connecting the Arctic to the North Atlantic via the Nordic Seas and the Greenland-Scotland Ridge. Arctic waters exit to the North Atlantic through the Fram Strait and the Davis Strait (~630 m) after transiting the CAA and Baffin Bay (Figure 1). Cold, fresher (~32.5), nutrient-rich Pacific water enters the Arctic through the shallow (~50 m) and narrow (~85 km) Bering Strait. The Arctic also receives a large amount of river water discharge (~4,300 km^3 yr^{-1}; Shiklomanov et al., 2021) in addition to the fresher Pacific water and freshwater stored in sea ice.

Incoming surface and intermediate Atlantic waters in the eastern Arctic are generally divided into the Polar Mixed Layer (PML, depth ~0–80 m, $S < 31$, $-1.8 < \theta < 1.8$°C), the Fram Strait Branch (FSB, depth in Eurasian Basin ~100–700 m, $34.5 < S < 34.85$, $\theta > 0$°C), and the Barents Sea Branch (BSB, depth in Eurasian Basin ~1,000–1,200 m, $34.85 < S < 34.9$, $-0.15 < \theta < 0$°C) (Figure 1). These surface and intermediate waters flow cyclonically following bathymetry and can cross the Lomonosov Ridge (~1,870 m), which divides the western and eastern Arctic basins (Rudels et al., 1994; Woodgate et al., 2001; Schauer et al., 2002). In the western Arctic, the FSB and BSB are readily traceable by a maximum in temperature (>0°C) and a minimum in dissolved oxygen, respectively (Schauer et al., 2002). While the PML is formed and maintained by freshwater inputs and seasonal sea ice melt, the subsurface cold halocline layer present across the Arctic is formed by mixing between surface and intermediate waters and the injection of saline waters modified on the shelves (Anderson et al., 2013).

Northward-flowing Pacific water is modified by brine rejection during sea ice formation on the shallow Chukchi shelves (Aagaard et al., 1981). Cold, salty water is injected into the western Arctic cold halocline via eddies and shelf break currents. The upper halocline layer (UHL, ~50–150 m, $31 < S < 33.1$, $-1.5 < \theta < 0.4$°C) is found primarily in the Canada Basin and overlies the eastern Arctic-origin lower halocline layer (LHL, ~100–300 m, $33.1 < S < 34.7$, $-1.5 < \theta < 0.3$°C) and the FSB (~300–500 m in western Arctic) and BSB (~500–1,500 m) below (McLaughlin et al., 2004) (Figure 1). The UHL circulation is primarily cyclonic and is advected into the CAA through the M'Clure Strait, where it becomes "Arctic Water" (AW, $-1.6 < \theta < 0.8$°C and $25.1 < S < 34.8$). These waters mix with Atlantic-origin water in Baffin Bay—West Greenland Intermediate Water (WGIW; ~300–800 m; $S > 34.2$, $\theta > 1.3$°C)—that crosses the Davis Strait sill from the Labrador Sea (Tang et al., 2004; Colombo et al., 2019). However, Baffin Bay Deep Water (BBDW; $S \sim 34.5$, $-1 < \theta < 1$°C) origins are still under debate (Tang et al., 2004), but they are isolated from Atlantic waters.

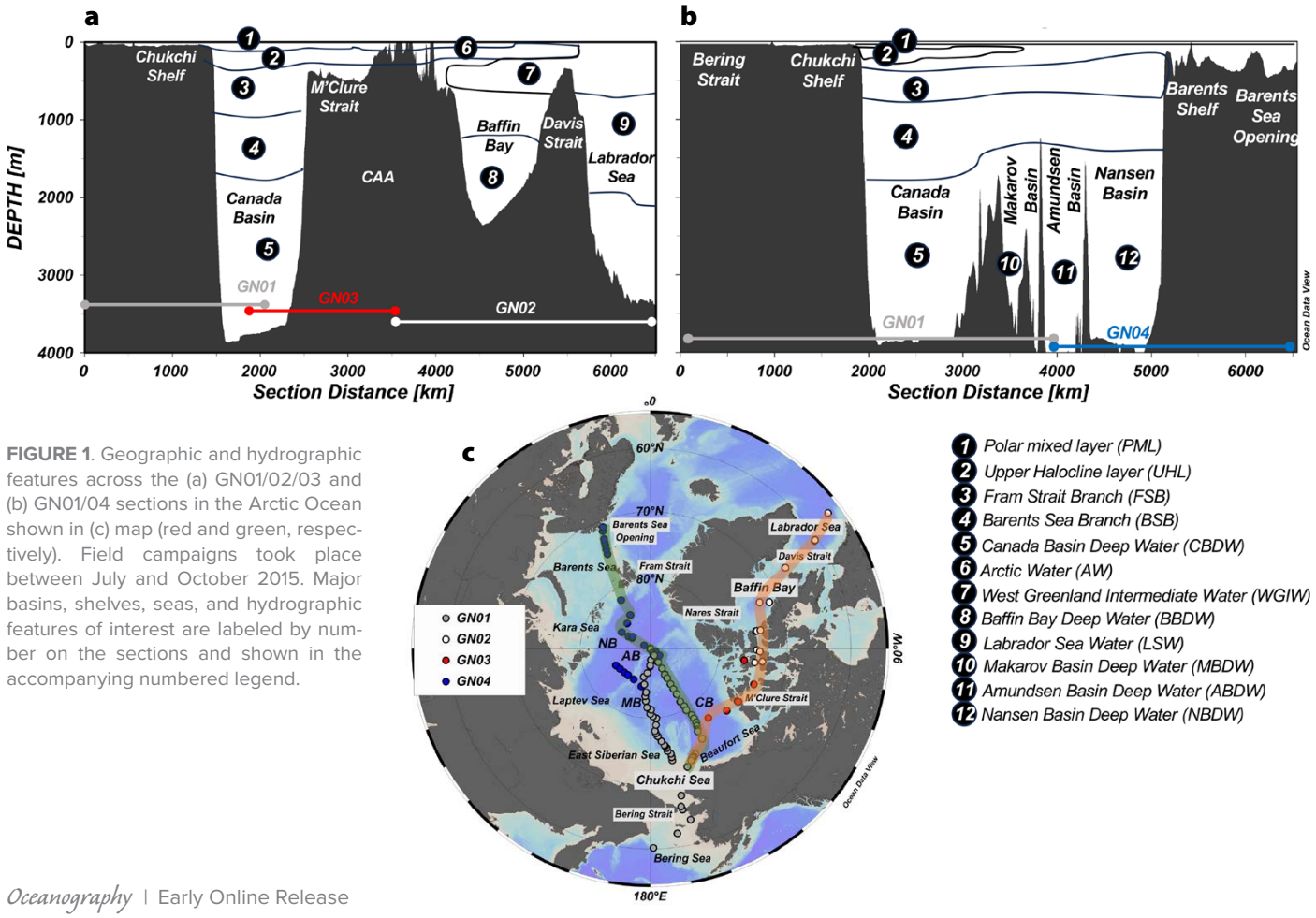

FIGURE 1. Geographic and hydrographic features across the (a) GN01/02/03 and (b) GN01/04 sections in the Arctic Ocean shown in (c) map (red and green, respectively). Field campaigns took place between July and October 2015. Major basins, shelves, seas, and hydrographic features of interest are labeled by number on the sections and shown in the accompanying numbered legend.

Arctic deep water (generally >1,200 m) movement is greatly restricted by ridge systems that form each sub-basin: the Alpha-Mendeleev Ridge (sill depth ~2,200 m) in the western Arctic, the Lomonosov Ridge, and the Gakkel Ridge (~2,500 m) in the eastern Arctic. The Fram Strait (~2,600 m) is the only point of deep water exchange in the Arctic; thus, the deep water masses are largely Atlantic in origin (Rudels, 2015).

TOWARD A PROCESS-ORIENTED FRAMEWORK EXPLAINING Fe AND Mn DISTRIBUTIONS

Shelf-Influenced Trace Metal Signature in Western and Canadian Arctic Ocean

The Chukchi Sea is a benthic-dominated shelf system: relatively fresh, summer sea ice melt and river-influenced surface waters create a stratified water column that keeps the post-bloom, late summer/early fall reservoir of nutrients and trace metals confined to the bottom waters (Granger et al., 2018). As the water column homogenizes in the winter, nutrients are mixed throughout the water column and help to stimulate production again in the spring (Pacini et al., 2019; Mordy et al., 2020). Pulses of organic carbon-rich export production to the sediments create a reducing environment within surface sediment that can stimulate the reductive dissolution of important trace metals such as Fe, Mn, Zn, Ni, Cu, and Cd, all of which are markedly elevated in Chukchi sediments (Cai et al., 2011; Vieira et al., 2019) and overlying bottom waters (Aguilar-Islas et al., 2013; Jensen et al., 2019, 2020; Zhang et al., 2019; Jensen et al., 2022). As a result, concentrations of dissolved trace metals in shelf bottom waters rival or exceed Pacific intermediate water concentrations, particularly for dFe and dMn (1,200% and 5,800% increase, respectively; Figure 2). This high dFe and dMn signature is then exported to the Canada Basin UHL through the Barrow Canyon (Aguilar-Islas et al., 2013). Other metals, such as Ni, Zn, and Cd, are indirectly solubilized during sediment diagenesis (described below) or during remineralization of trace metal-rich cells (Jensen et al., 2019). Freshwater contributes to the enhanced concentration of Cu and Ga over the Chukchi shelf, (Whitmore et al., 2020; Jensen et al., 2022) and of Fe, Cu, and Ni in the central Arctic, due to the river-influenced transpolar drift surface current (Charette et al., 2020), while V (Whitmore et al., 2019) and Pb (Colombo et al., 2019) are scavenged by the large particulate load present over this shallow shelf.

During the down-slope journey from the Canada Basin to the Labrador Sea and the North subarctic Atlantic, the trace element signature of the UHL undergoes further geochemical modifications while transiting the shallow Canadian Arctic Archipelago. The CAA is a highly dynamic environment, consisting of an intricate network of islands and channels that link the deep Canada Basin to Baffin Bay through the Parry Channel, Nares Strait, and Jones Sound (sill depths: ~120, 220, and 125 m, respectively; Figure 1). Large contributions of freshwater inputs from small permafrost-underlined rivers and sea ice meltwater (Rogalla et al., 2022), enhanced sediment resuspension (Colombo et al., 2021; Rogalla et al., 2022), and the recirculation and mixing of Pacific- and Atlantic-derived waters (Colombo et al., 2019) modulate the distribution of trace metals, as well as macronutrients, in the CAA (Michel et al., 2015; Colombo et al., 2020; Grenier et al., 2022). However, the relative influence of these processes results in marked spatial differences between the deeper (~500–600 m) and less energetic western CAA and the shallower

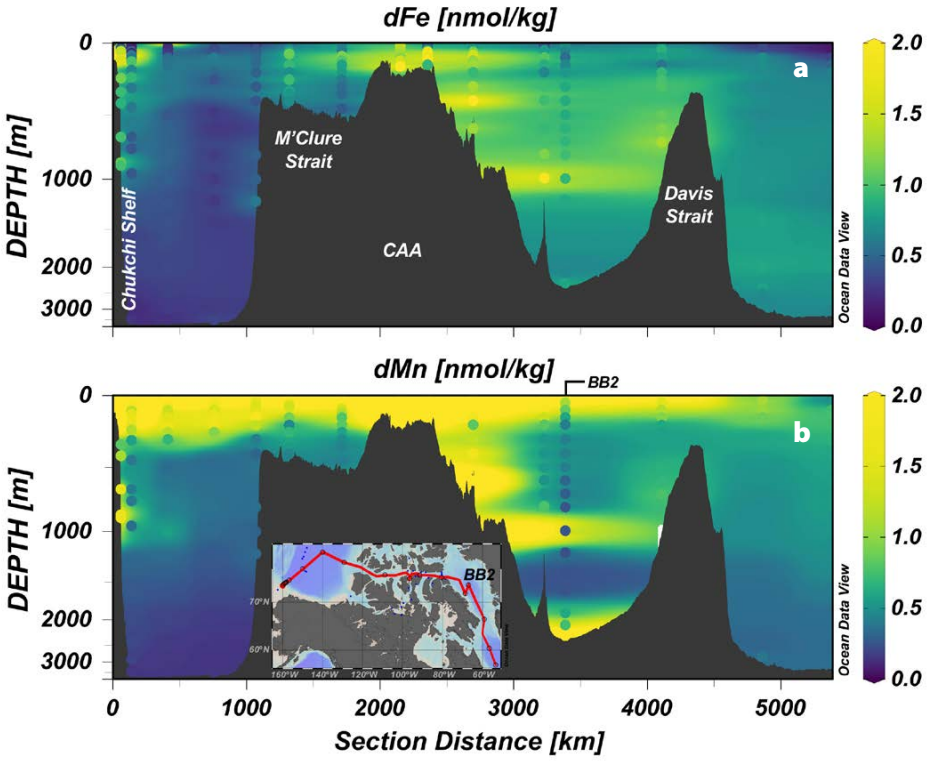

FIGURE 2. Dissolved (a) Fe and (b) Mn concentrations along the combined GN01 and GN02/03 sections sampled between July and October 2015. Concentrations are represented as both a background gridded product (weighted-average gridding) and actual measured sample concentrations (colored dots) following the same color scale. It is worth noting that the gridding at station BB2 (labeled) display artificially higher values (e.g., plume at ~1,000 m) than measured samples as this is the only deep station (>1,000 m) sampled in Baffin Bay, which is not part of the same circulation pathway as the rest of the gridded transect. The transect (shown in the inset map) begins at station 61 (GN01) on the Chukchi Shelf and ends at station K1 (GN02) in the Labrador Sea. Stations GN03 and GN02 in the Canadian Arctic Archipelago (CAA) were chosen to represent the outflow from the Arctic into Baffin Bay (Colombo et al., 2019). Please refer to Figure 1 for more geographic details. Note that the y-axis (depth) is stretched to emphasize the surface and subsurface distributions.

(~200–400 m) and more energetic eastern CAA. For instance, the concentrations of key bioactive trace metals such as Mn and Fe were up to 900% lower in the western CAA (e.g., dFe Min-Max range: 0.447–1.15 nmol kg^{-1}) than in the eastern CAA (e.g., dFe: 2.01–5.13 nmol kg^{-1}; Figure 2), where sediment resuspension is highest; this phenomenon is also described for other trace elements as well (e.g., V, Al; Colombo et al., 2021). The spatial distribution of other trace metals, such as Ga and Pb, is governed by the advection of Pacific-derived halocline water imprinting a low dGa and dPb signature (<10 pmol kg^{-1}) in western CAA and along the southern side of Parry Channel, whereas Baffin Bay waters of Atlantic origin with higher dGa and dPb concentrations recirculates along the northern side of Parry Channel (Colombo et al., 2019).

Similar near-bottom enrichment of Fe and Mn has been described for the Chukchi Shelf and the CAA, the two main gateways of Pacific-derived waters into the Arctic and North Atlantic Oceans, respectively. However, the processes, and thus the extent of the enrichment and advective transport, behind the benthic increase in trace metal concentrations differ greatly between these extensive and shallow shelf domains. The primary production levels, bathymetry, circulation, tidal forcing, and mixing strength in the Chukchi Sea and the CAA are anticipated to differentially influence Fe and Mn biogeochemistry in these regions.

In the Chukchi Sea, the rapid vertical export of organic material to the benthos (Lalande et al., 2021), and the consequential remineralization, trigger strong sedimentary reducing conditions, as evidenced by nitrogen isotope ratios and N* ($([NO_3^-] - 16 \times [PO_4^{3-}]) \times 0.87$)—a quasi-conservative tracer of denitrification/nitrification dynamics (Brown et al., 2015; Granger et al., 2018). Under these conditions, redox-sensitive elements such as Fe and Mn oxides undergo reductive dissolution. Consequently, these trace metals exhibit a strong negative correlation with N*, where near-bottom waters yield the highest dFe and dMn concentrations (up to ~20 and 200 nmol kg^{-1}, respectively; Figure 2) along with the most negative N* values, indicative of denitrification and reducing conditions within sediments (Figure 3). The rapid oxidation kinetics of Fe(II) (Millero et al., 1987) leads to oxidation and precipitation of the upward-diffusing Fe(II) into the overlying oxygenated water within the shelf domain, yielding a significant enrichment of particulate Fe (i.e., authigenic oxides, up to ~2,200 nmol kg^{-1}) over its crustal abundance, when normalized by particulate Al (Figure 3). The large Fe oxide contributions (up to ~50% of total particulate Fe) persist across the Chukchi shelf (Figure 3; Jensen et al., 2020; Xiang and Lam, 2020).

The distributions of Fe and Mn are decoupled in the Chukchi Sea (Jensen et al., 2020). Abiotic Mn oxidation is kinetically slower and has a higher pH range than Fe (Morgan, 2005; Luther, 2010), and thus, microbes drive Mn oxidation in the ocean (Cowen and Silver,

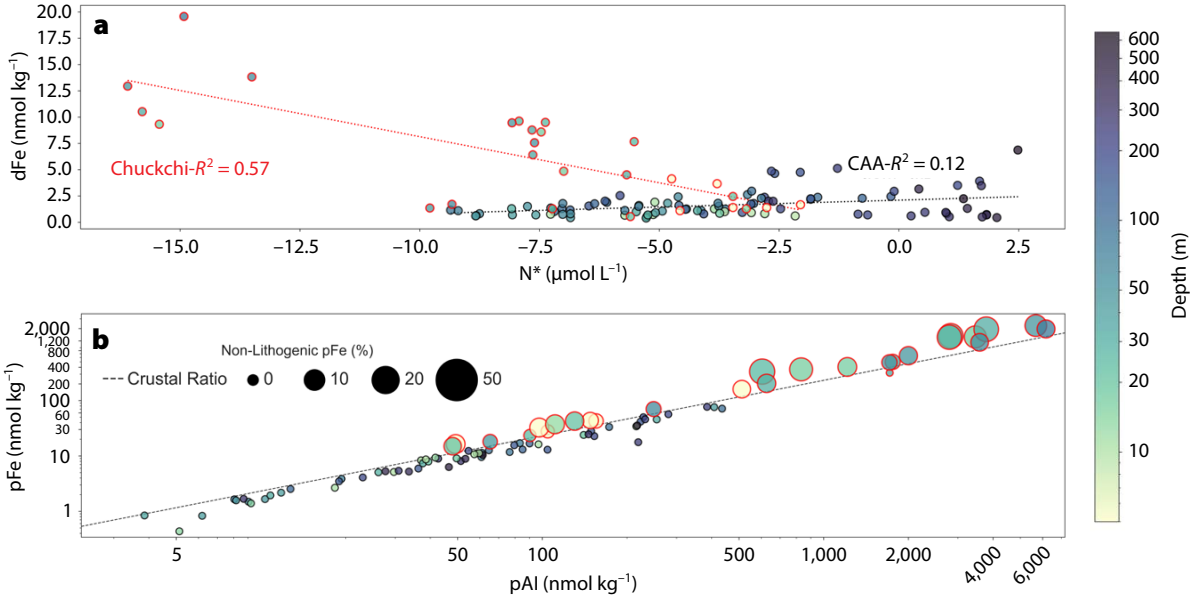

FIGURE 3. (a) dFe vs. N* in the Canadian Arctic Archipelago (CAA; black-edged circles and linear regression fit) and the Chukchi Shelf (red-edged circles and linear regression fit); dFe and N* data are from Colombo et al. (2020) and Jensen et al. (2020). (b) Relationship between pFe versus pAl in the CAA and Chukchi Shelf; note the logarithmic scale of the plot. The black-dashed line indicates the average upper continental crustal Fe:Al ratio from Rudnick and Gao (2003). Samples plotting above the crustal ratio are assumed to have variable non-lithogenic Fe oxide contributions (i.e., an excess of pFe over its lithogenic contribution). Non-lithogenic Fe oxide contributions are indicated by the symbol size; for details about the estimation of the non-lithogenic contribution, please refer to Xiang and Lam (2020). Particulate Fe, Al, and non-lithogenic Fe oxide data were retrieved from Jensen et al. (2020), Xiang and Lam (2020), and Colombo et al. (2021). All depths (color scale) from stations 3–6, 8, 9, 61, and 66 in the Chukchi Shelf and CAA1-CAA9 and CB1 in the CAA are included in these plots.

1984; Dick et al., 2006; Hansel, 2017). Both the slow abiotic kinetics of Mn(II) oxidation and potential photo-reductive dissolution of Mn oxides and photo-inhibition of Mn-oxidizing microbes (Sunda and Huntsman, 1988; Francis et al., 2001; Colombo et al., 2023) in the shallow Chukchi Shelf hinder oxidative processes. Consequently, Chukchi Shelf bottom waters are greatly enriched in dMn (up to ~200 nmol kg^{-1}), while pMn oxides are virtually absent.

Unlike the Chukchi shelf, the increase of Fe and Mn with depth and their near-bottom maxima in the shallow CAA shelf domain are not likely to be driven by strong reductive benthic supply but rather by enhanced sediment-water interaction and resuspension events (Colombo et al., 2021). In the CAA, primary production levels are high, albeit lower than in the Chukchi Sea (Hill et al., 2013); moreover, the relatively deeper CAA (~200 to 600 m vs. Chukchi Shelves ≤50 m) would allow for increased water column remineralization. Therefore, reduced vertical pulses of organic matter in the CAA together with strong mixing regimes (Hughes et al., 2017) and sediment resuspension events (Colombo et al., 2021), which result in the oxygenation of the seafloor, are expected to dampen sedimentary redox cycling (Lehmann et al., 2022). In fact, more positive N* values in the CAA are measured in near-bottom waters (Figure 3), while overlying Pacific-derived waters carry the reducing signature from Chukchi sediments. Other lines of evidence that point toward a non-reductive dissolution source of Fe and Mn in the CAA concern the lack of relationship between dFe and N* that was observed in the Chukchi Shelf. Lastly, the pFe/pAl relationship for all the samples in the CAA, unlike the Chukchi Shelf, displays near-crustal values (i.e., dominance of lithogenic contributions and virtual absence of Fe oxides; Figure 3). Enhanced shelf-ocean interactions in the CAA are sustained by strong tidal flow, shear instabilities, and internal waves breaking over the rough topography (Hughes et al., 2017). These phenomena lead to an increase of sediment resuspension events in the central sills area and eastern CAA region, favoring the desorption/dissolution of Fe and Mn as well as other trace metals, and thus explaining the Fe and Mn increase toward the bottom (Colombo et al., 2021).

Pacific-derived waters transiting the shallow shelf domains ventilate the subsurface halocline structure and retain their geochemical properties (e.g., macronutrients and trace metals) far from the shelves into the Arctic Ocean interior (Mathis et al., 2007). In the Canada Basin and Baffin Bay, the Fe and Mn signature of the subsurface UHL is modified along the flow path, depending on environmental conditions, oxidation kinetics, ligand stabilization, and microbial composition. In the Chukchi Sea, large benthic inputs of dFe are rapidly removed from the water column by authigenic Fe oxide formation as result of its fast oxidation kinetics under most oceanic water conditions (e.g., pH and redox potential; Luther, 2010). Although diminished, authigenic precipitation further reduces the dFe signature in halocline waters in the Canada Basin shelf break and slope regions, leading to a rapid offshore loss of dFe from the shelf domain (~10–20 nmol kg^{-1}; Jensen et al., 2020) and shelf break/slope areas (~0.8–4.5 nM; Hioki et al., 2014; Kondo et al., 2016; Jensen et al., 2020), to ~0.7 nmol kg^{-1} measured in the Canada Basin interior (Colombo et al., 2020; Jensen et al., 2020).

Although the high benthic dMn concentration is attenuated across the shelf transport into the ocean interior, the rate and spatial extent of scavenging removal and Mn oxide formation differ from that of Fe. Unlike Fe, most of the dMn exported from the Chukchi Shelf domain is removed from the water column offshore, with concentrations rapidly dropping to less than ~2 nmol kg^{-1} in the slope and across the entire Canada Basin (Kondo et al., 2016; Colombo et al., 2020; Jensen et al., 2020). Subsurface halocline waters (i.e., UHL: ~50–150 m) advected from the Chukchi Shelf have favorable environmental conditions, such as low light intensity, which alleviates bacterial photoinhibition and Mn oxide photoreduction, and high dissolved Mn concentrations, which boost Mn-oxidizing microbial dynamics and Mn oxidation (Colombo et al., 2023). The Mn oxide peak in halocline waters is a ubiquitous feature owing to its slow sinking rate and the relatively short timescale circulation of this water mass in the Canada Basin (<3 years from the slope to the basin interior; Colombo et al., 2023). The rapid loss of dMn and the bacterially mediated Mn oxide precipitation over the slope and in the ocean interior are indeed recorded in the benthos, where sediments within the Chukchi shelves are characterized by low and lithogenic-derived pMn, transitioning to sediments greatly enriched in non-lithogenic Mn (i.e., Mn oxides) in the slope region (Macdonald and Gobeil, 2012).

Similar processes as those described for the Chukchi Shelf and the Canada Basin operate in the CAA and Baffin Bay, where the high Fe and Mn outflow from the CAA is advected to the Baffin Bay interior (Colombo et al., 2023; Colombo et al., 2021; Figure 2). However, differences in the trace metal supply between the CAA and the Chukchi Shelf (non-reductive vs. reductive dissolution) influence the degree of Fe and Mn enrichment and oxide precipitation in the former region (Colombo et al., 2021). Another distinction between these two shelf-ocean systems is the extent of offshore dFe transported by subsurface halocline waters to the ocean interior (a distance over which concentrations drop to 1/e of the initial values; Johnson et al., 1997); it is 5 to 20 times greater in Baffin Bay (~1,450 km; Colombo et al., 2020) than in the Canada and Nansen basins (74–380 km and 260 km, respectively (Aguilar-Islas et al., 2013; Jensen et al., 2020; Klunder et al., 2012b). This discrepancy in dFe offshore transport from the CAA to Baffin Bay may reflect the increased strength of the horizontal advection (i.e., current direction predominantly parallel to the

continental slope relative to sampled stations) and lateral inputs from the Baffin Bay slope, which contrast with the nearly perpendicular position of sampled station in the Canada and Nansen basins with regards to UHL circulation.

The decoupling of the Fe and Mn cycles and the spatially different dominance of oxidative processes (e.g., over the shelf vs ocean interior) also shape the distribution of other trace elements in the Arctic Ocean because of the high sorptive nature of oxide phases (Koschinsky and Hein, 2003; Tebo et al., 2004; Hein et al., 2017). For instance, the distributions of Pb and V (particle reactive elements) are largely influenced by authigenic oxide formation; over the Chukchi Shelf, dissolved Pb and V concentrations are reduced by their adsorption onto Fe oxides, while their particulate phases are enriched over their lithogenic contributions (Colombo et al., 2019; Whitmore et al., 2019). Once advected to the Canada Basin, the abundant authigenic Mn oxides present in subsurface halocline waters act as the primary sorption agents.

As described for the Chukchi Shelf, the Barents shelf is productive, resulting in elevated nutrients and trace metals in the shelf bottom waters (Middag et al., 2011; Gerringa et al., 2021). Data from the 2015 GEOTRACES GN04 cruise demonstrate an enrichment of dZn, dFe, and dMn in Barents shelf bottom waters that may be incorporated into the FSB, the warm core of Atlantic-origin waters, although concentrations are lower compared to the western Arctic (Gerringa et al., 2021). Unlike the Chukchi, however, the Barents shelf is relatively deep (~200–400 m), preventing the full water column convection stimulated by sea ice formation and brine rejection that exports dense, nutrient-rich waters off-shelf in the Canada Basin. Although some cold and salty nutrient-rich water may be exported through the St. Anna trough in the Barents Sea, it is not enough to generate the same nutrient-rich cold halocline seen in the Canada Basin basins (Anderson et al., 2013). As a result, the Nansen and Amundsen trace metal distributions appear markedly different compared to the Chukchi-derived Canada and Makarov basin distributions (Figure 4).

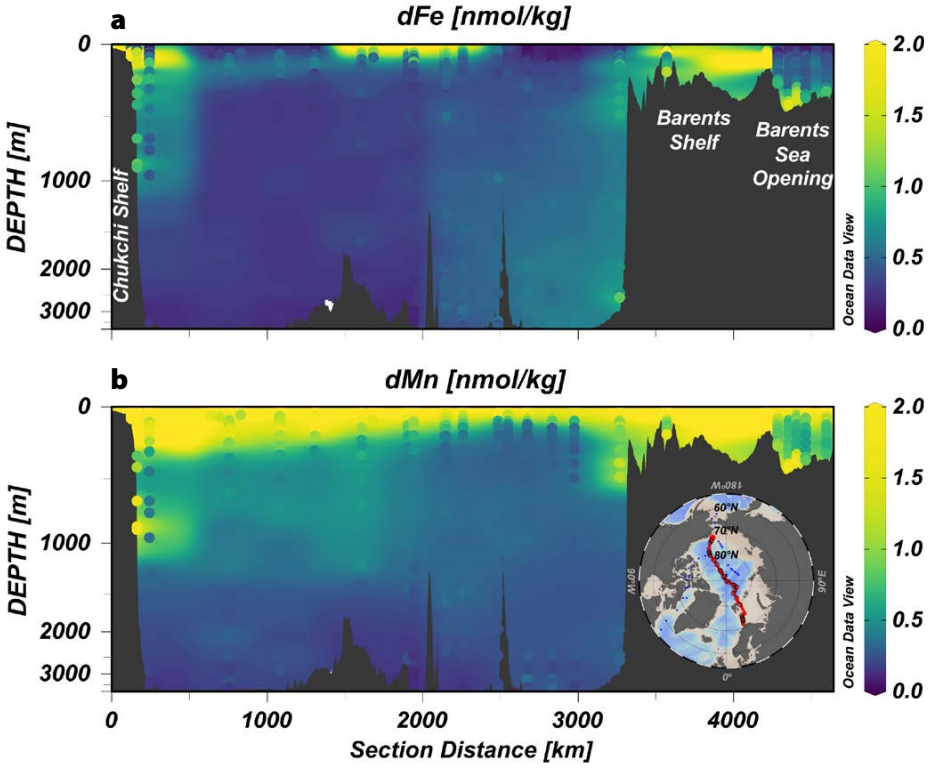

FIGURE 4. Dissolved (a) Fe and (b) Mn concentrations along the combined GN01 and GN04 sections. Concentrations are represented as both a background gridded product and sample dots following the same color scale. The transect (shown in the inset map) begins at station 61 (GN01) on the Chukchi Shelf and ends at station 169 (GN04) in the Barents Sea Opening (Gerringa et al., 2021; Jensen et al., 2022). Please refer to Figure 1 for more geographic details. Note that the y-axis (depth) is stretched to emphasize the distribution in the surface and subsurface.

Fe and Mn in Intermediate Waters (~300–1,000 m): Advective Transport as a Significant Source of Lithogenic-Derived Trace Metals

Below subsurface waters (>200–300 m), complex processes (e.g., advective transport, organic matter remineralization, scavenging) and ocean ridge systems modulate the geochemistry of trace metals including Fe and Mn, leading to distinct distributions across the Eurasian Arctic Basin, the Canada Basin, Baffin Bay, and the Labrador Sea (Figure 5). Advective transport of dissolved and particulate trace metals not only is a preeminent mechanism shaping their distributions in surface and subsurface Arctic waters (previous section) but also plays a significant role below the UHL, given the strong topographically stirred boundary currents of Atlantic-derived water masses entering the Arctic Ocean (Rudels et al., 1999; Tang et al., 2004; Aksenov et al., 2011). These boundary currents entrain lithogenic-derived trace elements, due to their close interaction with continental slope sediments while traveling around the rim of the Arctic Ocean, resulting in an elevated geochemical signature in the ocean interior. However, this source term is attenuated and/or increased by co-occurring processes, such as scavenging and remineralization of organic matter. For instance, scavenging removal reduces the comparatively high dFe concentrations (~0.5–0.6 nmol kg^{-1}) of the Atlantic Layer in Figure 1, FSB and BSB combined) in the eastern Arctic basin, along their cyclonic circulation from eastern Nansen Basin, to Amundsen Basin, to the isolated Makarov Basin, as they move away from slope sedimentary sources

(Figure 4; Gerringa et al., 2021; Klunder et al., 2012b; Middag et al., 2011).

Similarly, in the Canada Basin, the spatial and vertical distribution of dFe in the Atlantic Layer is largely shaped by the competing advective transport of this bioactive element from shelf-slope sediments and scavenging, while the contributions of organic matter remineralization and release of Fe to the water column are negligible (Figure 5; Colombo et al., 2020; Jensen et al., 2020). This is not surprising, as primary production and export production levels are low compared to those in other shelf systems and deep basins (Hill et al., 2013; Varela et al., 2013; Colombo et al., 2022;). Spatially, dFe concentrations in the Canada Basin Atlantic Layer reveal clear differences between those stations directly impacted by the Atlantic Layer (0.4–0.5 nmol kg^{-1}) close to the slope and those in the Canada Basin interior (0.25–0.30 nmol kg^{-1}; Figures 2 and 4). The variable influence of entrained sedimentary Fe by the Atlantic Layer below halocline waters is also seen in pFe, with spatial distributions mimicking dFe, and by pV and pAl (Colombo et al., 2022).

Advective transport also controls the distributions of Fe in the WGIW in Baffin Bay and in LSW; however, organic matter remineralization also contributes to the dFe pool in these water masses. A small, but still significant, difference in WGIW dFe concentrations is observed between the continental slope and sills areas (0.9–1.0 nmol kg^{-1}) and the interior of Baffin Bay (0.75–0.90 nmol kg^{-1}; Figure 2) due to the influence of intense cyclonic boundary currents closely interacting with the continental margin in the former regions (Colombo et al., 2022; Tang et al., 2004). A similar pattern is described for particulate Fe, Al, and V, emphasizing the importance of boundary processes that influence the distributions of lithogenic-derived trace metals in intermediate-depth waters.

Baffin Bay and Labrador Sea waters, unlike the Canada Basin, are highly productive, sustaining large phytoplankton blooms (Lehmann et al., 2019; Varela et al., 2013), and therefore, the remineralization (i.e., microbial degradation) of particulate organic matter below the euphotic zone represents an additional source term of Fe to the dissolved phase. Strong positive correlations between dFe concentrations and apparent oxygen utilization (a proxy of organic matter remineralization extent) across the entire WGIW highlights the prevalence of this additional source of dFe (Colombo et al., 2020). In Baffin Bay's interior, the influence of advective transport and organic matter remineralization as source terms of dFe, and other metals, is somewhat muted due to increased scavenging (Colombo et al., 2020).

In the Labrador Sea, a key region of deep-water formation, the dFe and dMn signature of intermediate waters (i.e., Labrador Sea Water, ~140–2,600 m) is largely shaped by sediment-water interactions/boundary transport, and microbial degradation of sinking organic matter (Yashayaev et al., 2007; Colombo et al., 2022), albeit the magnitude of such processes is lesser than in Baffin Bay (Figure 2). Indeed, sedimentary inputs appear to be a prevalent source term of dFe during the Labrador Sea Water southward flow, as the concentrations measured across the ~1,500 km transect from the North

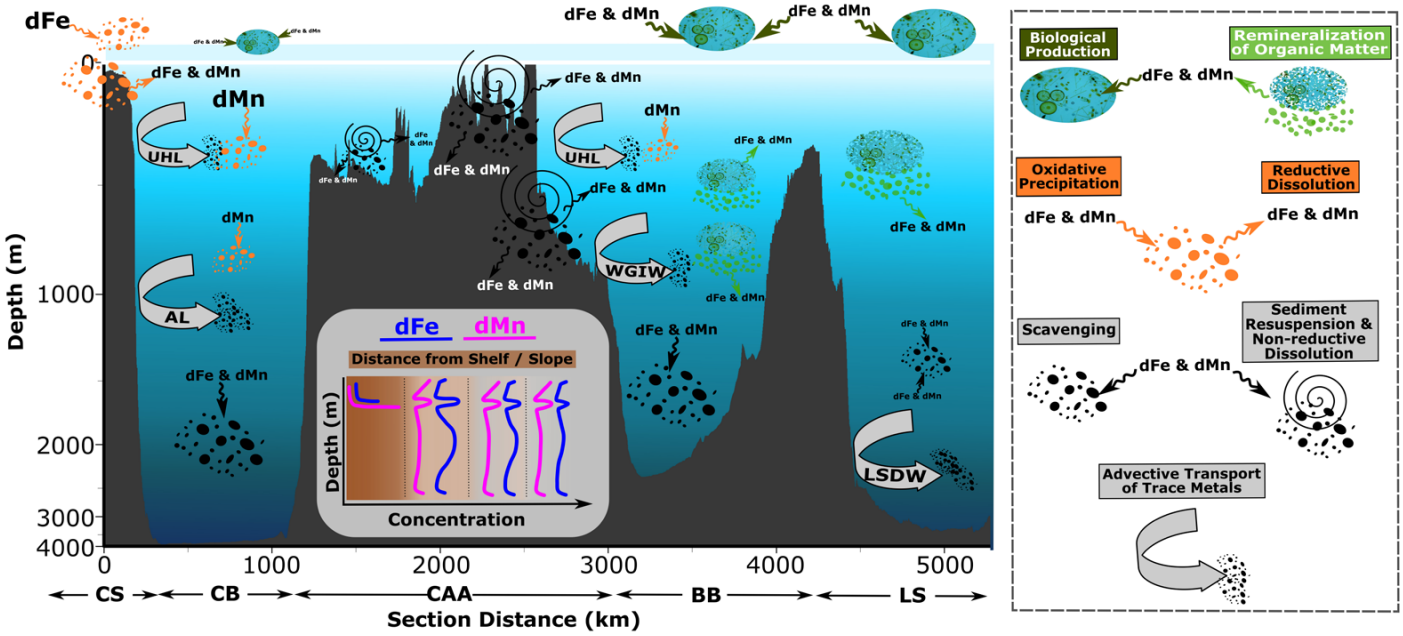

FIGURE 5. Conceptual summary of the key processes shaping dissolved Fe and Mn (dFe and dMn) from the Chukchi Shelf to the Labrador Sea. The sizes of label fonts and symbols represent the relative importance of described processes. CS = Chukchi Shelf. CB = Canada Basin. CAA = Canadian Arctic Archipelago. BB = Baffin Bay. LS = Labrador Sea. UHL = Upper Halocline Layer. AL = Atlantic Layer. WGIW = West Greenland Intermediate Water. LSDW = Labrador Sea Deep Water.

American Continental slope to the Bermuda Atlantic Time-series Study (BATS) station are higher than those of Labrador Sea Water (Fitzsimmons et al., 2015; Hatta et al., 2015; Colombo et al., 2020). Furthermore, the distinctively lighter dFe isotopic signature of this water mass along the North American margin supports the sediment-water interactions thesis, pointing toward non-reductive dissolution processes as the plausible source of Fe (Conway and John, 2014).

The Puzzling Behavior of Mn

An intriguing aspect of Mn biogeochemical cycling emerges in the western Arctic Ocean and Baffin Bay: the advective contributions of shelf and slope-derived lithogenic material and the biogenic component—assimilation and remineralization of dMn by aquatic primary producers and microbes—seem to be masked by strong oxidative precipitation and dissolution processes. Below halocline waters, the prevalent one-dimensional vertical dynamic of dMn sharply contrasts with that of dFe. Unlike dFe, the proportional influence of boundary currents does not provide a clear explanation for dMn across Atlantic-derived waters in the Canada Basin (~350–1,200 m) and, to a lesser extent, in Baffin Bay (~300–800 m). Distribution with depth is consistent between the continent shelf and slope regions and the basin interior (Figures 4 and 5). A similar pattern has been described for pMn, with nearly uniform concentration across the Canada Basin reflecting little influence of circumpolar boundary transport beyond the shelf domain (Colombo et al., 2022). This singular behavior of Mn in Canada Basin and Baffin Bay intermediate-depth waters is hypothesized to be driven by the overwhelming dominance of Mn oxides and the predominance of subsequent adsorption/desorption redox cycling in these basins, which contrast with the much lower contribution of Mn oxides and prevalent advective nature of dMn (i.e., more lithogenic-derived) in the LSW (Figure 5).

Fe and Mn in the Deep Waters (>1,200 m): Extended Scavenging Removal vs. Advective and Hydrothermal Sources

The geochemistry of dFe and dMn in the deep Canada Basin and Baffin Bay waters is largely shaped by their unique topographical settings, as both are isolated from lateral advective processes by complex ridge systems (Figure 5). The horizontal exchange of water masses at depths greater than 1,000–1,500 m is greatly restricted by the Alpha-Mendeleev Ridge (sill depth along the crest: ~1,000–2,400 m) and Davis Strait in the Canada Basin and Baffin Bay, respectively, which isolate the Canada Basin Deep Waters (CBDW) and Baffin Bay Deep Waters (BBDW) from boundary currents. Consequently, both the CBDW and BBDW have long residence times (500 and 360–690 years, respectively; Tanhua et al., 2009; Zeidan et al., 2022). Under these conditions, scavenging removal of dFe and dMn surpasses potential remineralization sources, resulting in a progressive reduction of their concentrations with depth (Figure 2). Low background levels are reached in the CBDW (dFe: ~0.24 nmol kg^{-1} and dMn: ~0.15 nmol kg^{-1}) and BBDW (dFe: ~0.65 nmol kg^{-1} and dMn: ~0.24 nmol kg^{-1})—not accounting for local benthic inputs (Colombo et al., 2020; Jensen et al., 2020).

Likewise, scavenging removal also controls the distributions of numerous dissolved trace metals (e.g., Zn, Cu, Ga) in the CBDW, Makarov Basin Deep Water (MBDW), and BBDW (McAlister and Orians, 2015; Jensen et al., 2022). This general decreasing trend in concentrations with depth is attenuated in the Labrador Sea deep waters (depth >2,000 m), where dFe and dMn (dFe: 0.65–0.81 nmol kg^{-1} and dMn: 0.31–0.38 nmol kg^{-1}) never reached the low levels of CBDW and BBDW (Figure 2). This behavior is likely explained by the much shorter ventilation age (<15 years; Azetsu-Scott et al., 2005) of Labrador Sea deep waters, which reduces the scavenging removal effect, and by the potential competing source of dFe and dMn along the flow path of this energetic deep water boundary current, which interacts with the bathymetry (Figure 5; Yashayaev et al., 2007; Colombo et al., 2022).

The Makarov Basin shares similar topographical features to those described for the Canada Basin and Baffin Bay, such as being separated from the Canada Basin by the Alpha-Mendeleev Ridge and from the Amundsen Basin by the Lomonosov Ridge, and thus, deep waters in the Makarov Basin are old (>400 years old) and largely isolated from advective transport (Tanhua et al., 2009). Considering the isolation and old age of MBDW, it is not surprising that scavenging has been suggested as the main mechanism behind the consistently low concentrations of dFe and dMn (Figure 4), as well as other trace metals, in these deep waters (Middag et al., 2011; Klunder et al., 2012b; Gerringa et al., 2021; Jensen et al., 2022). In the Nansen and Amundsen Basins, diffuse inputs of trace metals via shelf-slope convection (Roeske et al., 2012) and ongoing water exchange with the Greenland Sea, along with the hydrothermal point source of dFe and dMn at the Gakkel Ridge, seem to outcompete scavenging in the deep waters, which display higher concentrations of these elements compared to other Arctic basins (Figures 2 and 4; Middag et al. 2011; Klunder et al. 2012; Gerringa et al. 2021).

CONCLUDING REMARKS AND FUTURE WORK: Fe AND Mn BIOGEOCHEMISTRY IN THE ARCTIC OCEAN AND CLIMATE CHANGE

The GEOTRACES Arctic Program illuminated the complex, and often disparate, processes that shape the biogeochemistry of important micronutrients such as dFe and dMn, as well as other trace metals, in this unique environment (Figure 5). Given the disproportionate influence of freshwater sources, land-ocean interaction, advective transport, and sea ice dynamics controlling dFe and dMn distribution in the Arctic Ocean, it is expected

that climate change will have profound impacts on their cycling. Indeed, the biogeochemical response to a rapidly changing climate is well under way across the Arctic. In the western Arctic, changes range from the physical to biological, with an emphasis on increased primary production and shifting phytoplankton community composition (Li et al., 2009; Macdonald et al., 2015; Huntington et al., 2020; Lewis et al., 2020; Lalande et al., 2021). Sea ice retreat may lead to earlier and more intense spring blooms dependent on light availability. As a result, the flux of organic carbon to the seafloor may be more intense but less sustained over time (Lalande et al., 2021). Thus, the accumulation of Fe and Mn among other trace metals may be reduced over time in the Chukchi and Bering sediments. Reductive dissolution of Fe and Mn from these sediments is likely to be sustained under increasing nitrate deficit suggested by complementary tracers such as N* (Zhuang et al., 2022).

Moreover, warming and freshening of the Pacific inflow (Woodgate and Peralta-Ferriz, 2021) has increased over the past decade, leading to potential shoaling of the Chukchi shelf outflow that ventilates and sustains the Canada Basin UHL. As the UHL is a major reservoir for Fe, Mn, and macronutrients alike, a change in depth could bring important nutrients to the surface and sustain new productivity. Freshwater input is also likely to increase and enhance stratification across the Arctic (Nummelin et al., 2016). Increased freshwater can potentially bring more metals, such as Fe and Mn, which are rich in Arctic rivers (Charette et al., 2020; Kipp et al., 2020), into the central Arctic and the Fram Strait outflow. However, increased stratification may prohibit mixing and result in less upwelling of subsurface nutrients, which is not counteracted by wind-driven mixing (Peralta-Ferriz and Woodgate, 2015).

Freshwater accumulation in Baffin Bay may weaken the pressure gradient driving Arctic waters through the CAA and thus weaken Arctic-CAA-Atlantic exchange (Nummelin et al., 2016). Land-sea interactions such as submarine groundwater discharge are expected to increase due to melting permafrost, potentially remobilizing trace metals in affected areas such as the CAA (Guimond et al., 2022). Increased meltwater inputs from glaciers are likely to enhance nutrients and trace metals via direct supply or by promoting upwelling, leading to ephemeral blooms (Bhatia et al., 2021). As sea ice retreats, stratification will increase due to freshening and tidal stress in CAA bottom waters, which may be enhanced in the absence of dampening, resulting in increased physical resuspension of sediments (Rotermund et al., 2021). Thus, we may see large inputs of Fe and Mn from glaciers and sediments in the CAA and Baffin Bay that remain isolated from the surface and join the outflow to intermediate and deep waters in the Labrador Sea.

REFERENCES

Aagaard, K., L. Coachman, and E. Carmack. 1981. On the halocline of the Arctic Ocean. *Deep Sea Research Part A* 28(6):529–545, https://doi.org/10.1016/0198-0149(81)90115-1.

Aguilar-Islas, A.M., R. Rember, S. Nishino, T. Kikuchi, and M. Itoh. 2013. Partitioning and lateral transport of iron to the Canada Basin. *Polar Science* 7(2):82–99, https://doi.org/10.1016/j.polar.2012.11.001.

Aksenov, Y., V.V. Ivanov, A.G. Nurser, S. Bacon, I.V. Polyakov, A.C. Coward, A.C. Naveira-Garabato, and A. Beszczynska-Moeller. 2011. The Arctic circumpolar boundary current. *Journal of Geophysical Research: Oceans* 116(C9), https://doi.org/10.1029/2010JC006637.

Anderson, L.G., P.S. Andersson, G. Björk, E.P. Jones, S. Jutterström, and I. Wåhlström. 2013. Source and formation of the upper halocline of the Arctic Ocean. *Journal of Geophysical Research: Oceans* 118(1):410–421, https://doi.org/10.1029/2012JC008291.

Azetsu-Scott, K., E.P. Jones, and R.M. Gershey. 2005. Distribution and ventilation of water masses in the Labrador Sea inferred from CFCs and carbon tetrachloride. *Marine Chemistry* 94(1–4):55–66, https://doi.org/10.1016/j.marchem.2004.07.015.

Barnhart, K.R., C.R. Miller, I. Overeem, and J.E. Kay. 2016. Mapping the future expansion of Arctic open water. *Nature Climate Change* 6(3):280–285, https://doi.org/10.1038/nclimate2848.

Bhatia, M.P., S. Waterman, D.O. Burgess, P.L. Williams, R.M. Bundy, T. Mellett, M. Roberts, and E.M. Bertrand. 2021. Glaciers and nutrients in the Canadian Arctic Archipelago marine system. *Global Biogeochemical Cycles* 35(8):e2021GB006976, https://doi.org/10.1029/2021GB006976.

Brown, Z.W., K.L. Casciotti, R.S. Pickart, J.H. Swift, and K.R. Arrigo. 2015. Aspects of the marine nitrogen cycle of the Chukchi Sea shelf and Canada Basin. *Deep Sea Research Part II* 118:73–87, https://doi.org/10.1016/j.dsr2.2015.02.009.

Bruland, K.W., R. Middag, and M.C. Lohan. 2014. Controls of trace metals in seawater. Pp. 19–51 in *Treatise on Geochemistry* (Second Edition). H.D. Holland and K.K. Turekian, eds, Elsevier, Oxford, https://doi.org/10.1016/B978-0-08-095975-7.00602-1.

Cai, M.H., J. Lin, Q.Q. Hong, Y. Wang, and M.G. Cai. 2011. Content and distribution of trace metals in surface sediments from the northern Bering Sea, Chukchi Sea and adjacent Arctic areas. *Marine Pollution Bulletin* 63(5):523–527, https://doi.org/10.1016/j.marpolbul.2011.02.007.

Carmack, E., P. Winsor, and W. Williams. 2015. The contiguous panarctic Riverine Coastal Domain: A unifying concept. *Progress in Oceanography* 139:13–23, https://doi.org/10.1016/j.pocean.2015.07.014.

Charette, M.A., L.E. Kipp, L.T. Jensen, J.S. Dabrowski, L.M. Whitmore, J.N. Fitzsimmons, T. Williford, A. Ulfsbo, E. Jones, R.M. Bundy, and others. 2020. The Transpolar Drift as a source of riverine and shelf-derived trace elements to the central Arctic Ocean. *Journal of Geophysical Research: Oceans* 125:e2019JC015920, https://doi.org/10.1029/2019JC015920.

Colombo, M., B. Rogalla, P.G. Myers, S.E. Allen, and K.J. Orians. 2019. Tracing dissolved lead sources in the Canadian Arctic: Insights from the Canadian GEOTRACES program. *ACS Earth and Space Chemistry* 3(7):1,302–1,314, https://doi.org/10.1021/acsearthspacechem.9b00083.

Colombo, M., S.L. Jackson, J.T. Cullen, and K.J. Orians. 2020. Dissolved iron and manganese in the Canadian Arctic Ocean: On the biogeochemical processes controlling their distributions. *Geochimica et Cosmochimica Acta* 277:150–174, https://doi.org/10.1016/j.gca.2020.03.012.

Colombo, M., B. Rogalla, J. Li, S.E. Allen, K.J. Orians, and M.T. Maldonado. 2021. Canadian Arctic Archipelago shelf-ocean interactions: A major iron source to Pacific derived waters transiting to the Atlantic. *Global Biogeochemical Cycles* 35(10):e2021GB007058, https://doi.org/10.1029/2021GB007058.

Colombo, M., J. Li, B. Rogalla, S.E. Allen, and M.T. Maldonado. 2022. Particulate trace element distributions along the Canadian Arctic GEOTRACES section: Shelf-water interactions, advective transport and contrasting biological production. *Geochimica et Cosmochimica Acta* 323:183–201, https://doi.org/10.1016/j.gca.2022.02.013.

Colombo, M., J. LaRoche, D. Desai, J. Li, and M.T. Maldonado. 2023. Control of particulate manganese (Mn) cycling in halocline Arctic Ocean waters by putative Mn-oxidizing bacterial dynamics. *Limnology and Oceanography* 68(9):2,070–2,087, https://doi.org/10.1002/lno.12407.

Conway, T.M., and S.G. John. 2014. Quantification of dissolved iron sources to the North Atlantic Ocean. *Nature* 511(7508):212–215, https://doi.org/10.1038/nature13482.

Cowen, J.P., and M.W. Silver. 1984. The association of iron and manganese with bacteria on marine macroparticulate material. *Science* 224(4655):1,340–1,342, https://doi.org/10.1126/science.224.4655.1340.

Danielsson, L.-G., and S. Westerlund. 1983. Trace metals in the Arctic Ocean. Pp. 85–95 in *Trace Metals in Sea Water*. C.S. Wong, E. Boyle, K.W. Bruland, J.D. Burton, and E.D. Goldberg, eds, Springer US, Boston, MA, https://doi.org/10.1007/978-1-4757-6864-0_5.

Dick, G.J., Y.E. Lee, and B.M. Tebo. 2006. Manganese(II)-oxidizing *Bacillus* spores in Guaymas Basin hydrothermal sediments and plumes. *Applied and Environmental Microbiology* 72(5):3,184–3,190, https://doi.org/10.1128/AEM.72.5.3184-3190.2006.

Fitzsimmons, J.N., G.G. Carrasco, J. Wu, S. Roshan, M. Hatta, C.I. Measures, T.M. Conway, S.G. John, and E.A. Boyle. 2015. Partitioning of dissolved iron and iron isotopes into soluble and colloidal

phases along the GA03 GEOTRACES North Atlantic Transect. *Deep Sea Research Part II* 116:130–151, https://doi.org/10.1016/j.dsr2.2014.11.014.
Francis, C.A., E.-M. Co, and B.M. Tebo. 2001. Enzymatic manganese(II) oxidation by a marine α-proteobacterium. *Applied and Environmental Microbiology* 67(9):4,024–4,029, https://doi.org/10.1128/AEM.67.9.4024-4029.2001.
Frey, K.E., and J.W. McClelland. 2009. Impacts of permafrost degradation on Arctic river biogeochemistry. *Hydrological Processes* 23(1):169–182, https://doi.org/10.1002/hyp.7196.
Gerringa, L.J.A., M.J.A. Rijkenberg, H.A. Slagter, P. Laan, R. Paffrath, D. Bauch, M. Rutgers van der Loeff, and R. Middag. 2021. Dissolved Cd, Co, Cu, Fe, Mn, Ni and Zn in the Arctic Ocean. *Journal of Geophysical Research: Oceans* 126(9):e2021JC017323, https://doi.org/10.1029/2021JC017323.
Granger, J., D.M. Sigman, J. Gagnon, J.-E. Tremblay, and A. Mucci. 2018. On the properties of the Arctic halocline and deep water masses of the Canada Basin from nitrate isotope ratios. *Journal of Geophysical Research: Oceans* 123(8):5,443–5,458, https://doi.org/10.1029/2018JC014110.
Grenier, M., K. Brown, M. Colombo, M. Belhadj, I. Baconnais, V. Pham, M. Soon, P. Myers, C. Jeandel, and R. François. 2022. Controlling factors and impacts of river-borne neodymium isotope signatures and rare earth element concentrations supplied to the Canadian Arctic Archipelago. *Earth and Planetary Science Letters* 578:117341, https://doi.org/10.1016/j.epsl.2021.117341.
Guimond, J.A., A.A. Mohammed, M.A. Walvoord, V.F. Bense, and B.L. Kurylyk. 2022. Sea-level rise and warming mediate coastal groundwater discharge in the Arctic. *Environmental Research Letters* 17(4):045027, https://doi.org/10.1088/1748-9326/ac6085.
Hansel, C.M. 2017. Manganese in marine microbiology. *Advances in Microbial Physiology* 70:37–83, https://doi.org/10.1016/bs.ampbs.2017.01.005.
Hatta, M., C.I. Measures, J. Wu, S. Roshan, J.N. Fitzsimmons, P. Sedwick, and P. Morton. 2015. An overview of dissolved Fe and Mn distributions during the 2010–2011 US GEOTRACES North Atlantic cruises: GEOTRACES GA03. *Deep Sea Research Part II* 116:117–129, https://doi.org/10.1016/j.dsr2.2014.07.005.
Hein, J.R., N. Konstantinova, M. Mikesell, K. Mizell, J.N. Fitzsimmons, P.J. Lam, L.T. Jensen, Y. Xiang, A. Gartman, G. Cherkashov, and others. 2017. Arctic deep water ferromanganese-oxide deposits reflect the unique characteristics of the Arctic Ocean. *Geochemistry, Geophysics, Geosystems* 18(11):3,771–3,800, https://doi.org/10.1002/2017GC007186.
Hill, V.J., P.A. Matrai, E. Olson, S. Suttles, M. Steele, L.A. Codispoti, and R.C. Zimmerman. 2013. Synthesis of integrated primary production in the Arctic Ocean: Part II. In situ and remotely sensed estimates. *Progress in Oceanography* 110:107–125, https://doi.org/10.1016/j.pocean.2012.11.005.
Hioki, N., K. Kuma, Y. Morita, R. Sasayama, A. Ooki, Y. Kondo, H. Obata, J. Nishioka, Y. Yamashita, and S. Nishino. 2014. Laterally spreading iron, humic-like dissolved organic matter and nutrients in cold, dense subsurface water of the Arctic Ocean. *Scientific Reports* 4:6775, https://doi.org/10.1038/srep06775.
Holmes, R.M., A.I. Shiklomanov, A. Suslova, M. Tretiakov, J.W. McClelland, L. Scott, R.G.M. Spencer, and S.E. Tank. 2021. *River Discharge*. NOAA Technical Report OAR ARC; 21-11, 7 pp., https://doi.org/10.25923/zevf-ar65.
Hughes, K.G., J.M. Klymak, X. Hu, and P.G. Myers. 2017. Water mass modification and mixing rates in a 1/12° simulation of the Canadian Arctic Archipelago. *Journal of Geophysical Research: Oceans* 122(2):803–820, https://doi.org/10.1002/2016JC012235.
Huntington, H.P., S.L. Danielson, F.K. Wiese, M. Baker, P. Boveng, J.J. Citta, A. De Robertis, D.M.S. Dickson, E. Farley, J.C. George, and others. 2020. Evidence suggests potential transformation of the Pacific Arctic ecosystem is underway. *Nature Climate Change* 10(4):342–348, https://doi.org/10.1038/s41558-020-0695-2.
Jakobsson, M., A. Grantz, Y. Kristoffersen, R. Macnab, R. MacDonald, E. Sakshaug, R. Stein, and W. Jokat. 2004. The Arctic Ocean: Boundary conditions and background information. Pp. 1–32 in *The Organic Carbon Cycle in the Arctic Ocean*. R. Stein and R.W. MacDonald, eds, Springer, https://doi.org/10.1007/978-3-642-18912-8_1.
Jensen, L.T., N.J. Wyatt, B.S. Twining, S. Rauschenberg, W.M. Landing, R.M. Sherrell, and J.N. Fitzsimmons. 2019. Biogeochemical cycling of dissolved zinc in the western Arctic (Arctic GEOTRACES GN01). *Global Biogeochemical Cycles* 33(3):343–369, https://doi.org/10.1029/2018GB005975.
Jensen, L.T., P. Morton, B.S. Twining, M.I. Heller, M. Hatta, C.I. Measures, S. John, R. Zhang, P. Pinedo-Gonzalez, and R.M. Sherrell. 2020. A comparison of marine Fe and Mn cycling: US GEOTRACES GN01 Western Arctic case study. *Geochimica et Cosmochimica Acta* 288:138–160, https://doi.org/10.1016/j.gca.2020.08.006.
Jensen, L.T., J.T. Cullen, S.L. Jackson, L.J. Gerringa, D. Bauch, R. Middag, R.M. Sherrell, and J.N. Fitzsimmons. 2022. A refinement of the processes controlling dissolved copper and nickel biogeochemistry: Insights from the pan-Arctic. *Journal of Geophysical Research: Oceans* 127(5):e2021JC018087, https://doi.org/10.1029/2021JC018087.
John, S., and T. Conway. 2014. A role for scavenging in the marine biogeochemical cycling of zinc and zinc isotopes. *Earth and Planetary Science Letters* 394:159–167, https://doi.org/10.1016/j.epsl.2014.02.053.
Johnson, K.S., R.M. Gordon, and K.H. Coale. 1997. What controls dissolved iron concentrations in the world ocean? *Marine Chemistry 57*(3):137–161, https://doi.org/10.1016/S0304-4203(97)00043-1.
Kipp, L.E., P.B. Henderson, Z.A. Wang, and M.A. Charette. 2020. Deltaic and estuarine controls on Mackenzie River solute fluxes to the Arctic Ocean. *Estuaries and Coasts* 43(8):1,992–2,014, https://doi.org/10.1007/s12237-020-00739-8.
Klunder, M.B., D. Bauch, P. Laan, H.J.W. de Baar, S. van Heuven, and S. Ober. 2012a. Dissolved iron in the Arctic shelf seas and surface waters of the central Arctic Ocean: Impact of Arctic river water and ice-melt. *Journal of Geophysical Research: Oceans* 117(C1), https://doi.org/10.1029/2011JC007133.
Klunder, M.B., P. Laan, R. Middag, H.J.W. de Baar, and K. Bakker. 2012b. Dissolved iron in the Arctic Ocean: Important role of hydrothermal sources, shelf input and scavenging removal. *Journal of Geophysical Research: Oceans* 117(C4), https://doi.org/10.1029/2011JC007135.
Kondo, Y., H. Obata, N. Hioki, A. Ooki, S. Nishino, T. Kikuchi, and K. Kuma. 2016. Transport of trace metals (Mn, Fe, Ni, Zn and Cd) in the western Arctic Ocean (Chukchi Sea and Canada Basin) in late summer 2012. *Deep Sea Research Part I* 116:236–252, https://doi.org/10.1016/j.dsr.2016.08.010.
Koschinsky, A., and J.R. Hein. 2003. Uptake of elements from seawater by ferromanganese crusts: Solid-phase associations and seawater speciation. *Marine Geology* 198(3):331–351, https://doi.org/10.1016/S0025-3227(03)00122-1.
Lalande, C., J.M. Grebmeier, A.M. McDonnell, R.R. Hopcroft, S. O'Daly, and S.L. Danielson. 2021. Impact of a warm anomaly in the Pacific Arctic region derived from time-series export fluxes. *PLoS ONE* 16(8):e0255837, https://doi.org/10.1371/journal.pone.0255837.
Lehmann, N., M. Kienast, J. Granger, A. Bourbonnais, M. Altabet, and J.É. Tremblay. 2019. Remote western Arctic nutrients fuel remineralization in deep Baffin Bay. *Global Biogeochemical Cycles* 33(6):649–667, https://doi.org/10.1029/2018GB006134.
Lehmann, N., M. Kienast, J. Granger, and J.É. Tremblay. 2022. Physical and biogeochemical influences on nutrients through the Canadian Arctic Archipelago: Insights from nitrate isotope ratios. *Journal of Geophysical Research: Oceans* 127(3):e2021JC018179, https://doi.org/10.1029/2021JC018179.
Lewis, K.M., G.L. van Dijken, and K.R. Arrigo. 2020. Changes in phytoplankton concentration now drive increased Arctic Ocean primary production. *Science* 369(6500):198–202, https://doi.org/10.1126/science.aay8380.
Li, W.K., F.A. McLaughlin, C. Lovejoy, and E.C. Carmack. 2009. Smallest algae thrive as the Arctic Ocean freshens. *Science* 326(5952):539–539, https://doi.org/10.1126/science.1179798.
Luther, G.W. 2010. The role of one-and two-electron transfer reactions in forming thermodynamically unstable intermediates as barriers in multi-electron redox reactions. *Aquatic Geochemistry* 16:395–420, https://doi.org/10.1007/s10498-009-9082-3.
Macdonald, R.W., and C. Gobeil. 2012. Manganese sources and sinks in the Arctic Ocean with reference to periodic enrichments in basin sediments. *Aquatic Geochemistry* 18(6):565–591, https://doi.org/10.1007/s10498-011-9149-9.
Macdonald, R., Z. Kuzyk, and S. Johannessen. 2015. It is not just about the ice: A geochemical perspective on the changing Arctic Ocean. *Journal of Environmental Studies and Sciences* 5(3):288–301, https://doi.org/10.1007/s13412-015-0302-4.
Mathis, J.T., R.S. Pickart, D.A. Hansell, D. Kadko, and N.R. Bates. 2007. Eddy transport of organic carbon and nutrients from the Chukchi Shelf: Impact on the upper halocline of the western Arctic Ocean. *Journal of Geophysical Research: Oceans* 112(C5), https://doi.org/10.1029/2006JC003899.
McAlister, J.A., and K.J. Orians. 2015. Dissolved gallium in the Beaufort Sea of the western Arctic Ocean: A GEOTRACES cruise in the International Polar Year. *Marine Chemistry* 177:101–109, https://doi.org/10.1016/j.marchem.2015.05.007.
McLaughlin, F.A., E.C. Carmack, R.W. Macdonald, H. Melling, J.H. Swift, P.A. Wheeler, B.F. Sherr, and E.B. Sherr. 2004. The joint roles of Pacific and Atlantic-origin waters in the Canada Basin, 1997–1998. *Deep Sea Research Part I* 51(1):107–128, https://doi.org/10.1016/j.dsr.2003.09.010.
Michel, C., J. Hamilton, E. Hansen, D. Barber, M. Reigstad, J. Iacozza, L. Seuthe, and A. Niemi. 2015. Arctic Ocean outflow shelves in the changing Arctic: A review and perspectives. *Progress in Oceanography* 139:66–88, https://doi.org/10.1016/j.pocean.2015.08.007.
Middag, R., H.J.W. de Baar, P. Laan, and M.B. Klunder. 2011. Fluvial and hydrothermal input of manganese into the Arctic Ocean. *Geochimica et Cosmochimica Acta* 75(9):2,393–2,408, https://doi.org/10.1016/j.gca.2011.02.011.
Millero, F.J., S. Sotolongo, and M. Izaguirre. 1987. The oxidation kinetics of Fe(II) in seawater. *Geochimica et Cosmochimica Acta* 51(4):793–801, https://doi.org/10.1016/0016-7037(87)90093-7.
Moore, J., and O. Braucher. 2008. Sedimentary and mineral dust sources of dissolved iron to the world ocean. *Biogeosciences* 5(3):631–656, https://doi.org/10.5194/bg-5-631-2008.

Moore, R.M. 1981. Oceanographic distributions of zinc, cadmium, copper and aluminium in waters of the central Arctic. *Geochimica et Cosmochimica Acta* 45(12):2,475–2,482, https://doi.org/10.1016/0016-7037(81)90099-5.

Moore, R., M.G. Lowings, and F. Tan. 1983. Geochemical profiles in the central Arctic Ocean: Their relation to freezing and shallow circulation. *Journal of Geophysical Research: Oceans* 88(C4):2,667–2,674, https://doi.org/10.1029/JC088iC04p02667.

Mordy, C.W., S. Bell, E.D. Cokelet, C. Ladd, G. Lebon, P. Proctor, P. Stabeno, D. Strausz, E. Wisegarver, and K. Wood. 2020. Seasonal and interannual variability of nitrate in the eastern Chukchi Sea: Transport and winter replenishment. *Deep Sea Research Part II* 177:104807, https://doi.org/10.1016/j.dsr2.2020.104807.

Morel, F.M.M. 2008. The co-evolution of phytoplankton and trace element cycles in the oceans. *Geobiology* 6(3):318–324, https://doi.org/10.1111/j.1472-4669.2008.00144.x.

Morgan, J.J. 2005. Kinetics of reaction between O_2 and Mn(II) species in aqueous solutions. *Geochimica et Cosmochimica Acta* 69(1):35–48, https://doi.org/10.1016/j.gca.2004.06.013.

Nummelin, A., M. Ilicak, C. Li, and L.H. Smedsrud. 2016. Consequences of future increased Arctic runoff on Arctic Ocean stratification, circulation, and sea ice cover. *Journal of Geophysical Research: Oceans* 121(1):617–637, https://doi.org/10.1002/2015JC011156.

Opsahl, S., R. Benner, and R.M.W. Amon. 1999. Major flux of terrigenous dissolved organic matter through the Arctic Ocean. *Limnology and Oceanography* 44(8):2,017–2,023, https://doi.org/10.4319/lo.1999.44.8.2017.

Pacini, A., G.W.K. Moore, R.S. Pickart, C. Nobre, F. Bahr, K. Våge, and K.R. Arrigo. 2019. Characteristics and transformation of Pacific winter water on the Chukchi Sea shelf in late spring. *Journal of Geophysical Research: Oceans* 124(10):7,153–7,177, https://doi.org/10.1029/2019JC015261.

Peralta-Ferriz, C., and R.A. Woodgate. 2015. Seasonal and interannual variability of pan-Arctic surface mixed layer properties from 1979 to 2012 from hydrographic data, and the dominance of stratification for multiyear mixed layer depth shoaling. *Progress in Oceanography* 134:19–53, https://doi.org/10.1016/j.pocean.2014.12.005.

Perovich, D.K., and J.A. Richter-Menge. 2015. Regional variability in sea ice melt in a changing Arctic. *Philosophical Transactions of the Royal Society A* 373(2045), https://doi.org/10.1098/rsta.2014.0165.

Roeske, T., M. Rutgers van der Loeff, R. Middag, and K. Bakker. 2012. Deep water circulation and composition in the Arctic Ocean by dissolved barium, aluminium and silicate. *Marine Chemistry* 132:56–67, https://doi.org/10.1016/j.marchem.2012.02.001.

Rogalla, B., S.E. Allen, M. Colombo, P.G. Myers, and K.J. Orians. 2022. Sediments in sea ice drive the Canada Basin surface Mn maximum: Insights from an Arctic Mn ocean model. *Global Biogeochemical Cycles* 36(8):e2022GB007320, https://doi.org/10.1029/2022GB007320.

Rotermund, L.M., W.J. Williams, J.M. Klymak, Y. Wu, R.K. Scharien, and C. Haas. 2021. The effect of sea ice on tidal propagation in the Kitikmeot Sea, Canadian Arctic Archipelago. *Journal of Geophysical Research: Oceans* 126(5):e2020JC016786, https://doi.org/10.1029/2020JC016786.

Rudels, B., E.P. Jones, L.G. Anderson, and G. Kattner. 1994. On the intermediate depth waters of the Arctic Ocean. Pp. 33–46 in *The Polar Oceans and Their Role in Shaping the Global Environment*. O.M. Johannessen, R.D. Muench, and J.E. Overland, eds, American Geophysical Union, Washington, DC, https://doi.org/10.1029/GM085p0033.

Rudels, B., H.J. Friedrich, and D. Quadfasel. 1999. The Arctic circumpolar boundary current. *Deep Sea Research Part II* 46(6–7):1,023–1,062, https://doi.org/10.1016/S0967-0645(99)00015-6.

Rudels, B. 2015. Arctic Ocean circulation, processes and water masses: A description of observations and ideas with focus on the period prior to the International Polar Year 2007–2009. *Progress in Oceanography* 132:22–67, https://doi.org/10.1016/j.pocean.2013.11.006.

Rudnick, R., and S. Gao. 2003. Composition of the continental crust. Pp. 1–64 in *Treatise on Geochemistry,* vol. 3. D. Holland and K.K. Turekian, eds, https://doi.org/10.1016/B0-08-043751-6/03016-4.

Schauer, U., B. Rudels, E. Jones, L. Anderson, R. Muench, G. Björk, J. Swift, V. Ivanov, and A.-M. Larsson. 2002. Confluence and redistribution of Atlantic water in the Nansen, Amundsen and Makarov basins. *Annales Geophysicae* 20(2):257–273, https://doi.org/10.5194/angeo-20-257-2002.

Shiklomanov, A., S. Déry, M. Tretiakov, D. Yang, D. Magritsky, A. Georgiadi, and W. Tang. 2021. River freshwater flux to the Arctic Ocean. Pp. 703–738 in *Arctic Hydrology, Permafrost and Ecosystems*, D. Yang and D. L. Kane, eds, Springer International Publishing.

Sunda, W.G., and S.A. Huntsman. 1988. Effect of sunlight on redox cycles of manganese in the southwestern Sargasso Sea. *Deep Sea Research Part A* 35(8):1,297–1,317, https://doi.org/10.1016/0198-0149(88)90084-2.

Tang, C.C., C.K. Ross, T. Yao, B. Petrie, B.M. DeTracey, and E. Dunlap. 2004. The circulation, water masses and sea-ice of Baffin Bay. *Progress in Oceanography* 63(4):183–228, https://doi.org/10.1016/j.pocean.2004.09.005.

Tanhua, T., E.P. Jones, E. Jeansson, S. Jutterström, W.M. Smethie, D.W.R. Wallace, and L.G. Anderson. 2009. Ventilation of the Arctic Ocean: Mean ages and inventories of anthropogenic CO_2 and CFC-11. *Journal of Geophysical Research: Oceans* 114(C1), https://doi.org/10.1029/2008JC004868.

Tebo, B.M., J.R. Bargar, B.G. Clement, G.J. Dick, K.J. Murray, D. Parker, R. Verity, and S.M. Webb. 2004. Biogenic manganese oxides: Properties and mechanisms of formation. *Annual Review of Earth and Planetary Sciences* 32(1):287–328, https://doi.org/10.1146/annurev.earth.32.101802.120213.

Twining, B.S., and S.B. Baines. 2013. The trace metal composition of marine phytoplankton. *Annual Review of Marine Science* 5:191–215, https://doi.org/10.1146/annurev-marine-121211-172322.

Varela, D.E., D.W. Crawford, I.A. Wrohan, S.N. Wyatt, and E.C. Carmack. 2013. Pelagic primary productivity and upper ocean nutrient dynamics across Subarctic and Arctic Seas. *Journal of Geophysical Research: Oceans* 118(12):7,132–7,152, https://doi.org/10.1002/2013JC009211.

Vieira, L.H., E.P. Achterberg, J. Scholten, A.J. Beck, V. Liebetrau, M.M. Mills, and K.R. Arrigo. 2019. Benthic fluxes of trace metals in the Chukchi Sea and their transport into the Arctic Ocean. *Marine Chemistry* 208:43–55, https://doi.org/10.1016/j.marchem.2018.11.001.

Whitmore, L.M., P.L. Morton, B.S. Twining, and A.M. Shiller. 2019. Vanadium cycling in the western Arctic Ocean is influenced by shelf-basin connectivity. *Marine Chemistry* 216:103701, https://doi.org/10.1016/j.marchem.2019.103701.

Whitmore, L.M., A. Pasqualini, R. Newton, and A.M. Shiller. 2020. Gallium: A new tracer of Pacific Water in the Arctic Ocean. *Journal of Geophysical Research: Oceans* 125(7):e2019JC015842, https://doi.org/10.1029/2019JC015842.

Woodgate, R.A., K. Aagaard, R.D. Muench, J. Gunn, G. Björk, B. Rudels, A.T. Roach, and U. Schauer. 2001. The Arctic Ocean Boundary Current along the Eurasian slope and the adjacent Lomonosov Ridge: Water mass properties, transports and transformations from moored instruments. *Deep Sea Research Part I* 48(8):1,757–1,792, https://doi.org/10.1016/S0967-0637(00)00091-1.

Woodgate, R.A., and C. Peralta-Ferriz. 2021. Warming and freshening of the Pacific inflow to the Arctic from 1990–2019 implying dramatic shoaling in Pacific Winter Water ventilation of the Arctic water column. *Geophysical Research Letters* 48(9):e2021GL092528, https://doi.org/10.1029/2021GL092528.

Xiang, Y., and P.J. Lam. 2020. Size-fractionated compositions of marine suspended particles in the Western Arctic Ocean: Lateral and vertical sources. *Journal of Geophysical Research: Oceans* 125(8):e2020JC016144, https://doi.org/10.1029/2020JC016144.

Yashayaev, I., H.M. van Aken, N.P. Holliday, and M. Bersch. 2007. Transformation of the Labrador Sea Water in the subpolar North Atlantic. *Geophysical Research Letters* 34(22), https://doi.org/10.1029/2007GL031812.

Yeats, P.A. 1988. Manganese, nickel, zinc and cadmium distributions at the Fram-3 and Cesar ice camps in the Arctic Ocean. *Oceanologica Acta* 11(4):383–388.

Zeidan, S., J. Walker, B.G. Else, L.A. Miller, K. Azetsu-Scott, and B.D. Walker. 2022. Using radiocarbon measurements of dissolved inorganic carbon to determine a revised residence time for deep Baffin Bay. *Frontiers in Marine Science* 9:845536, https://doi.org/10.3389/fmars.2022.845536.

Zhang, R., L.T. Jensen, J.N. Fitzsimmons, R.M. Sherrell, and S. John. 2019. Dissolved cadmium and cadmium stable isotopes in the western Arctic Ocean. *Geochimica et Cosmochimica Acta* 258:258–273, https://doi.org/10.1016/j.gca.2019.05.028.

Zhuang, Y., H. Jin, W.-J. Cai, H. Li, D. Qi, and J. Chen. 2022. Extreme nitrate deficits in the western Arctic Ocean: Origin, decadal changes, and implications for denitrification on a polar marginal shelf. *Global Biogeochemical Cycles* 36(7):e2022GB007304, https://doi.org/10.1029/2022GB007304.

AUTHORS

Laramie Jensen (jensenla@uw.edu) is Research Associate, Polar Science Center, Applied Physics Laboratory, University of Washington, Seattle, WA, USA. **Manuel Colombo** is Assistant Professor, Virginia Institute of Marine Science, Gloucester Point, VA, USA.

ARTICLE CITATION

Jensen, L., and M. Colombo. 2024. Shelf-basin connectivity drives dissolved Fe and Mn distributions in the western Arctic Ocean: A synoptic view into polar trace metal cycling. *Oceanography* 37(2), https://doi.org/10.5670/oceanog.2024.410.

COPYRIGHT & USAGE